J Braz. Soc. Mech. Sci. Eng. (2013) 35:381–389
DOI 10.1007/s40430-013-0036-8

TECHNICAL PAPER

Influence of thermal stratification on the radiative flow of Maxwell fluid

T. Hayat · S. A. Shehzad · Hamed H. Al-Sulami · S. Asghar

Received: 30 January 2013 / Accepted: 18 May 2013 / Published online: 8 June 2013

Abstract We carried out analysis of the effects of thermal stratification in the boundary layer mixed convection flow of Maxwell fluid. The thermal radiation effect is considered. The derived equations with appropriate boundary conditions are solved for series solutions of velocity and temperature. Graphical results lead to the interesting observations. Local Nusselt number is tabulated and discussed. It is found that there is an opposite effect of fluid characteristics on the velocity and temperature. However, the velocity and temperature have similar effects for thermal stratification and radiation.

Keywords Thermal stratification · Maxwell fluid · Mixed convection flow · Thermal radiation

1 Introduction

The dynamics of non-Newtonian fluids is of great interest amongst the recent researchers of both the theoretical and applied fields. This type of fluids cannot be explained by using Newton's law of viscosity. Many fluids such as polymer melts, mud, soaps, apple sauce, certain oils, lubricants, suspension solutions, ketchup and many others exhibit the rheological properties and thus cannot be described by one constitutive relationship. Therefore, the existing information regarding non-Newtonian fluids has been presented through the differential, rate and integral types. It is further seen that the rate type fluids are not given due attention. Maxwell fluid is a subclass of rate type fluids describing the relaxation time effects. Jamil and Fetecau [1] in a recent study reported an analysis for the helical flows of Maxwell fluid. They discussed the flow situation when the inner cylinder begins to rotate around its axis and to slide along the same axis due to time-dependent shear stresses. Hankel transform method is employed for the development of exact solution. Couette flow of fractional Maxwell fluid with accelerated shear rate was studied by Athar et al. [2]. Expressions for velocity and shear stress are obtained using Laplace and finite Hankel transforms. Wang and Tan [3] provided the stability analysis of Maxwell fluid with Soret-driven double diffusive convection in a porous medium. Hayat et al. [4] examined the flow of Maxwell fluid subject to convective boundary conditions. Thermophoresis effects in the two-dimensional flow of Maxwell fluid was analyzed by Hayat et al. [5]. Few other recent attempts involving Maxwell fluid model may be mentioned by the Refs. [6–10].

Mixed convection flow with heat transfer over a continuously moving surface is encountered in extrusion processes, cooling of metallic sheets and electronic chips, melt spinning, crystal blowing, continuous casting, glass blowing, etc. Further, mixed convection flow also has a pivotal role in the environment when the temperature difference between land and air leads to complicated flow patterns. Slip effects on the unsteady mixed convection flow over a moving surface was

Technical Editor: Francisco Ricardo Cunha.

T. Hayat · S. A. Shehzad (✉)
Department of Mathematics, Quaid-i-Azam University, 45320, Islamabad 44000, Pakistan
e-mail: ali_qau70@yahoo.com

T. Hayat · H. H. Al-Sulami
Department of Mathematics, Faculty of Science, King Abdulaziz University, Jeddah 21589, Saudi Arabia

S. Asghar
Department of Mathematics, COMSATS Institute of Information Technology, Park Road, Chak Shahzad, Islamabad 44000, Pakistan

examined by Mukhopadhyay [11]. Turkyilmazoglu [12] provided the analytic solutions for mixed hydrodynamic thermal slip flow past a stretching surface. Two-dimensional flow of viscous fluid over an inclined stretching surface was numerically investigated by Noor et al. [13]. Convective heat transfer in two-dimensional flow of Maxwell fluid over a non-isothermal stretching sheet was investigated by Vajravelu et al. [14]. Hayat and Alsaedi [15] studied the mixed convection boundary layer flow of an Oldroyd-B fluid over a moving surface. They explored the effects of thermophoresis and Joule heating. Simultaneous effects of heat and mass transfer in MHD mixed convection flow with porous medium and internal heat generation were studied by Makinde [16]. Series solutions for mixed convection Falkner-Skan flow of Maxwell fluid was addressed by Hayat et al. [17].

Thermal radiation effect has a vital role in operations carried out at high temperature. Such effect is particularly important in the industrial and engineering applications including nuclear power plant, satellites, missiles, propulsion devices for aircraft and other space vehicles. Further, the study of thermally stratified fluid is significant in various industrial, environment and engineering processes. In fact the thermal stratification is a property of all fluid bodies surrounded by differentially heated side walls [18]. Thermal stratification for vertical consideration is due to temperature variations, concentration difference or presence of different density fluids. Having such in mind, Kulkarni et al. [19] carried out a study to investigate the similarity solution over an isothermal vertical surface in a thermally stratified medium. Natural convection flow in a thermally stratified medium over a vertical cylinder was examined by Thakhar et al. [20]. Hossain et al. [21] discussed the effects of viscous dissipation and thermal stratification on the flow of viscous fluid in the presence of uniform surface heat flux. Singh et al. [22] examined the thermal stratification effects on MHD flow of viscous fluid. Recently, Mukhopadhyay and Ishak [23] provided the numerical solutions for the thermally stratified flow over a stretching cylinder.

To the best of our information, the boundary layer due to temperature gradient in non-Newtonian fluid with radiation effects has not been attained so far. This interest motivated us to examine such effects for the flow of Maxwell fluid over a stretched surface. This article is arranged in the following pattern. Next section deals with the definitions of problem and some physical quantities. Series solutions and related convergence analysis are given in the Sects. 3 and 4 respectively by homotopy analysis method [24–28]. Physical results are presented in Sect. 5. Section 6 contains main conclusions.

2 Governing problems

We consider the mixed convection flow of an incompressible Maxwell fluid over a stretching surface. Thermal stratification and radiation effects are present. The vertical surface has temperature T_w and further T_∞ denotes the temperature of ambient fluid. The x and y-axes are chosen along and normal to the surface. The equation of continuity, the equations of momentum in the absence of pressure gradient [6] and the equation of energy can be written as

$$\frac{\partial u}{\partial x}+\frac{\partial v}{\partial y}=0, \tag{1}$$

$$\rho\left(u\frac{\partial u}{\partial x}+v\frac{\partial u}{\partial y}\right)=\frac{\partial \tau_{xx}}{\partial x}+\frac{\partial \tau_{xy}}{\partial y}+g\beta_T(T-T_\infty), \tag{2}$$

$$\rho\left(u\frac{\partial v}{\partial x}+v\frac{\partial v}{\partial y}\right)=\frac{\partial \tau_{yx}}{\partial x}+\frac{\partial \tau_{yy}}{\partial y}, \tag{3}$$

$$\rho C_p\left(u\frac{\partial T}{\partial x}+v\frac{\partial T}{\partial y}\right)=k\frac{\partial^2 T}{\partial y^2}-\frac{\partial q_r}{\partial y}, \tag{4}$$

where u and v denote the velocity components in the x- and y-directions, ρ the fluid density, T the fluid temperature, k the thermal conductivity of fluid, g the gravitational acceleration, β_T the thermal expansion coefficient, C_p the specific heat at constant pressure and q_r the radiative heat flux. The extra stress tensor τ_{ij} related to the deformation rate tensor d_{ij} for a Maxwell fluid can be defined as [29]:

$$\tau_{ij}+\lambda\frac{\triangle}{\triangle t}\tau_{ij}=2\delta d_{ij}, \tag{5}$$

in which δ is the coefficient of viscosity, λ is the relaxation time and $\frac{\triangle}{\triangle t}$ is the upper convected time derivative. By applying this time derivative to the stress tensor, we have [29]

$$\frac{\triangle}{\triangle t}\tau_{ij}=\frac{D}{Dt}\tau_{ij}-L_{jk}\tau_{ik}-L_{ik}\tau_{kj}, \tag{6}$$

where L_{ij} denote the velocity gradient tensor. For an incompressible flow of Maxwell fluid, the x-component of the momentum equation and energy equation after employing the boundary layer theory [30] has the following forms:

$$u\frac{\partial u}{\partial x}+v\frac{\partial u}{\partial y}+\lambda_1\left(u^2\frac{\partial^2 u}{\partial x^2}+v^2\frac{\partial^2 u}{\partial y^2}+2uv\frac{\partial^2 u}{\partial x\partial y}\right)=\nu\frac{\partial^2 u}{\partial y^2}+g\beta_T(T-T_\infty), \tag{7}$$

$$\rho C_p\left(u\frac{\partial T}{\partial x}+v\frac{\partial T}{\partial y}\right)=k\frac{\partial^2 T}{\partial y^2}-\frac{\partial q_r}{\partial y}, \tag{8}$$

where ν is the kinematic viscosity. The subjected boundary conditions are

$$u=u_w(x)=cx,\ v=0,\ T=T_w=T_0+bx\ \text{ at }\ y=0, \tag{9}$$

$$u\to 0,\ T\to T_\infty=T_0+ax\quad \text{as}\ y\to\infty, \tag{10}$$

in which c is the stretching rate, a, b are dimensional constants and T_0 is the reference temperature.

The radiative flux is accounted by the Rosseland approximation in the energy equation [31]:

$$q_r = -\frac{4\sigma^*}{3k^*}\frac{\partial T^4}{\partial y}, \tag{11}$$

in which σ^* the Stefan-Boltzmann constant and k^* the mean absorption coefficient. Further, the differences of temperature within the flow is assumed to be small such that T^4 may be expressed as a linear function of temperature. Expansion of T^4 about T_∞ via Taylor's series and ignoring higher order terms, we have

$$T^4 \cong T_\infty^4 + (T - T_\infty)4T_\infty^3 = 4T_\infty^3 T - 3T_\infty^4. \tag{12}$$

By employing Eqs. (11) and (12), Eq. (8) has the form

$$\rho C_p\left(u\frac{\partial T}{\partial x} + v\frac{\partial T}{\partial y}\right) = k\frac{\partial^2 T}{\partial y^2} + \frac{16\sigma T_\infty^3}{3k^*}\frac{\partial^2 T}{\partial y^2}. \tag{13}$$

Setting

$$u = cxf'(\eta),\ v = -\sqrt{cv}f(\eta),\ \eta = y\sqrt{\frac{c}{v}},\ \theta(\eta) = \frac{T - T_\infty}{T_w - T_0}, \tag{14}$$

Equation (1) is satisfied automatically and reduced forms of Eqs. (7)–(10) and (13) are

$$f''' + ff'' - f'^2 + \beta(2ff'f'' - f^2 f''') + \lambda\theta = 0, \tag{15}$$

$$(1 + \frac{4}{3}N)\theta'' + Prf\theta' - Prf'\theta - PrSf' = 0, \tag{16}$$

and the boundary conditions in dimensionless form has the following form:

$$f = 0,\ f' = 1,\ \theta = 1 - S \quad \text{at } \eta = 0, \tag{17}$$

$$f' = 0,\ \theta = 0 \quad \text{as } \eta \to \infty. \tag{18}$$

Here $De = \lambda_1 c$ is the Deborah number, $\lambda = Gr_x/Re_x^2$ the mixed convection parameter with $Gr_x = g\beta_T(T - T_\infty)x^3/v^2$ the local Grashof number and $Re_x = u_w(x)x/v$ the local Reynolds number, $Pr = v/\alpha$ the Prandtl number, $\alpha = \frac{k}{\rho C_p}$ the thermal diffusivity, $N = \frac{4\sigma^* T_\infty^3}{kk^*}$ the thermal radiation parameter, $S = b/a$ the thermal stratification parameter, θ the dimensionless temperature and η the similarity variable.

Local Nusselt number is defined by

$$Nu_x = \frac{xq_w}{k(T - T_\infty)}, \tag{19}$$

where the heat transfer from the surface q_w is

$$q_w = -k\left(\frac{\partial T}{\partial y}\right)_{y=0}. \tag{20}$$

Equation (13) in dimensionless variables is given as

$$Nu_x/Re_x^{1/2} = -\theta'(0). \tag{21}$$

3 Development of the series solutions

For an interest in the homotopy analysis solutions we choose the initial guesses and operators in the form given below:

$$f_0(\eta) = (1 - \exp(-\eta)),\ \theta_0(\eta) = (1 - S)\exp(-\eta), \tag{22}$$

$$\mathcal{L}_f = f''' - f',\ \mathcal{L}_\theta = \theta'' - \theta, \tag{23}$$

with

$$\mathcal{L}_f(C_1 + C_2 e^\eta + C_3 e^{-\eta}) = 0,\ \mathcal{L}_\theta(C_4 e^\eta + C_5 e^{-\eta}) = 0, \tag{24}$$

where C_i (i = 1–5) are the arbitrary constants. The zeroth order deformation equations together with the boundary conditions are

$$(1 - p)\mathcal{L}_f\left(\hat{f}(\eta;p) - f_0(\eta)\right) = p\hbar_f\mathcal{N}_f\left(\hat{f}(\eta;p), \hat{\theta}(\eta;p)\right), \tag{25}$$

$$(1 - p)\mathcal{L}_\theta\left(\hat{\theta}(\eta;p) - \theta_0(\eta)\right) = p\hbar_\theta\mathcal{N}_\theta\left(\hat{f}(\eta;p), \hat{\theta}(\eta,p)\right), \tag{26}$$

$$\hat{f}(0;p) = 0, \hat{f}'(0;p) = 1, \hat{f}'(\infty;p) = 0,\ \hat{\theta}(0,p) = 1 - S,\ \hat{\theta}(\infty,p) = 0, \tag{27}$$

$$\mathcal{N}_f[\hat{f}(\eta,p)] = \frac{\partial^3\hat{f}(\eta,p)}{\partial\eta^3} + \hat{f}(\eta,p)\frac{\partial^2\hat{f}(\eta,p)}{\partial\eta^2} - \left(\frac{\partial\hat{f}(\eta,p)}{\partial\eta}\right)^2 + \lambda\hat{\theta}(\eta,p) \tag{28}$$

$$+De\left(2\hat{f}(\eta,q)\frac{\partial\hat{f}(\eta,q)}{\partial\eta}\frac{\partial^2\hat{f}(\eta,q)}{\partial\eta^2} - (\hat{f}(\eta,q))^2\frac{\partial^3\hat{f}(\eta,q)}{\partial\eta^3}\right), \tag{29}$$

$$\mathcal{N}_\theta[\hat{\theta}(\eta,p),\hat{f}(\eta,p)] = (1 + \frac{4}{3}N)\frac{\partial^2\hat{\theta}(\eta,p)}{\partial\eta^2} - Pr\hat{\theta}(\eta,p)\frac{\partial\hat{f}(\eta,p)}{\partial\eta} + Pr\hat{f}(\eta,p)\frac{\partial\hat{\theta}(\eta,p)}{\partial\eta} - PrS\frac{\partial\hat{f}(\eta,p)}{\partial\eta}, \tag{30}$$

where p is an embedding parameter, $\hbar_f$ and $\hbar_\theta$ the non-zero auxiliary parameters and $\mathcal{N}_f$ and $\mathcal{N}_\theta$ the nonlinear operators. For $p = 0$ and $p = 1$ one has

$$\hat{f}(\eta;0) = f_0(\eta),\ \hat{\theta}(\eta,0) = \theta_0(\eta) \text{ and } \hat{f}(\eta;1) = f(\eta),\ \hat{\theta}(\eta,1) = \theta(\eta). \tag{31}$$

When variation of p is taken into account from 0 to 1 then $f(\eta, p)$ and $\theta(\eta, p)$ vary from $f_0(\eta)$, $\theta_0(\eta)$ to $f(\eta)$ and $\theta(\eta)$. We expand f and θ in the following forms:

$$f(\eta,p) = f_0(\eta) + \sum_{m=1}^{\infty} f_m(\eta)p^m,\ f_m(\eta) = \frac{1}{m!}\frac{\partial^m f(\eta;p)}{\partial \eta^m}\bigg|_{p=0}, \tag{32}$$

$$\theta(\eta,p) = \theta_0(\eta) + \sum_{m=1}^{\infty} \theta_m(\eta)p^m,\ \theta_m(\eta) = \frac{1}{m!}\frac{\partial^m \theta(\eta;p)}{\partial \eta^m}\bigg|_{p=0}, \tag{33}$$

where the convergence of above series strongly depends upon $\hbar_f$ and $\hbar_\theta$. Considering that $\hbar_f$ and $\hbar_\theta$ are selected properly such that Eqs. (32) and (33) converge for $p = 1$ and thus

$$f(\eta) = f_0(\eta) + \sum_{m=1}^{\infty} f_m(\eta), \tag{34}$$

$$\theta(\eta) = \theta_0(\eta) + \sum_{m=1}^{\infty} \theta_m(\eta). \tag{35}$$

The general solutions are derived as follows:

$$f_m(\eta) = f_m^*(\eta) + C_1 + C_2e^{\eta} + C_3e^{-\eta} \tag{36}$$

$$\theta_m(\eta) = \theta_m^*(\eta) + C_4e^{\eta} + C_5e^{-\eta} \tag{37}$$

where f_m^* and θ_m^* are the special solutions.

4 Convergence analysis

The auxiliary parameters $\hbar_f$ and $\hbar_\theta$ appearing in the series solutions have the key role regarding the control and adjustment of the convergence of the homotopy solutions. Hence, the $\hbar$—curves are sketched for 21st order of approximations to find the range of admissible values of $\hbar_f$ and $\hbar_\theta$. It is obvious from Fig. 1 that the range of admissible values of $\hbar_f$ and $\hbar_\theta$ are $-1.15 \leq \hbar_f \leq -0.2$ and $-1.1 \leq \hbar_\theta \leq -0.15$. Both series are convergent in the whole region of η for $\hbar_f = -0.7$ and $\hbar_\theta = -0.6$.

5 Results and discussion

The purpose of this section is to describe the role of emerging parameters through plots and construction of tabular values of Nusselt number. Such objective is achieved for the variations of Deborah number De, mixed convection parameter λ, thermal stratified parameter S, Prandtl number Pr and radiation parameter N on the velocity $f'(\eta)$ and temperature $\theta(\eta)$. The effects of Deborah number on velocity and temperature are seen in the Figs. 2 and 3. We observed that the velocity and associated boundary layer thickness are decreased by increasing De. This is attributed to the fact that the relaxation time opposes the fluid flow. De is dependent on the relaxation time and an

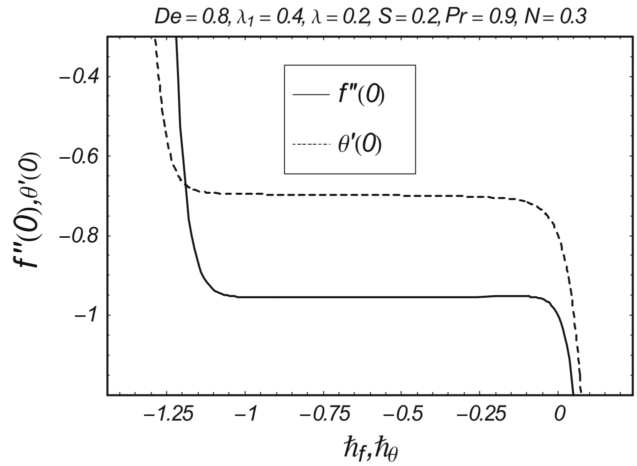

Fig. 1 $\hbar$ —curves for the functions $f(\eta)$ and θ (η)

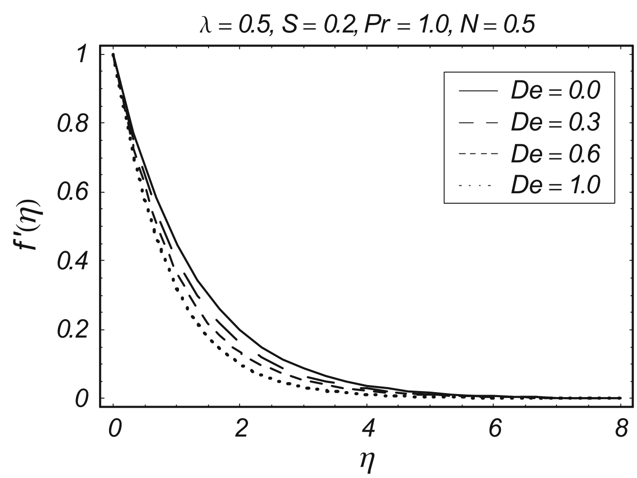

Fig. 2 Influence of De on $f'(\eta)$

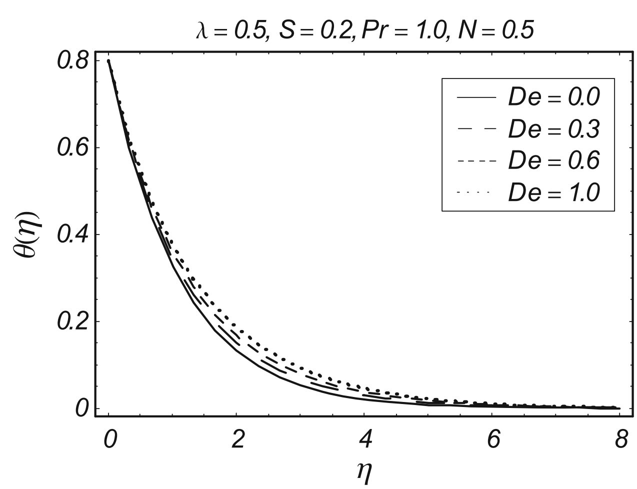

Fig. 3 Influence of De on $\theta(\eta)$

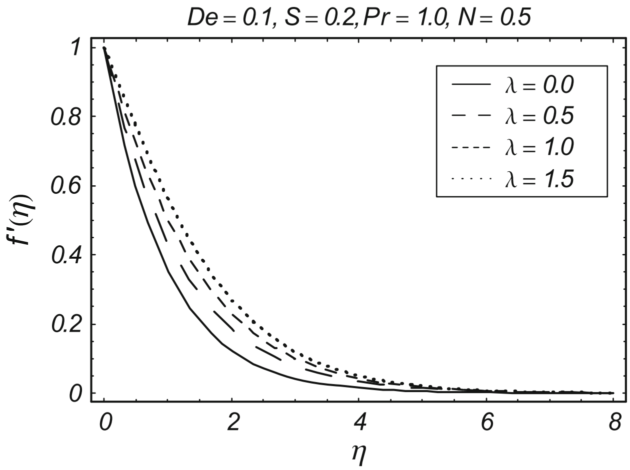

Fig. 4 Influence of λ on $f'(\eta)$

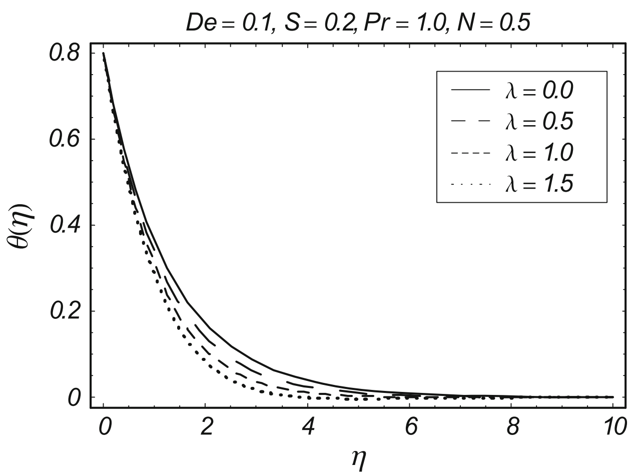

Fig. 5 Influence of λ on $\theta(\eta)$

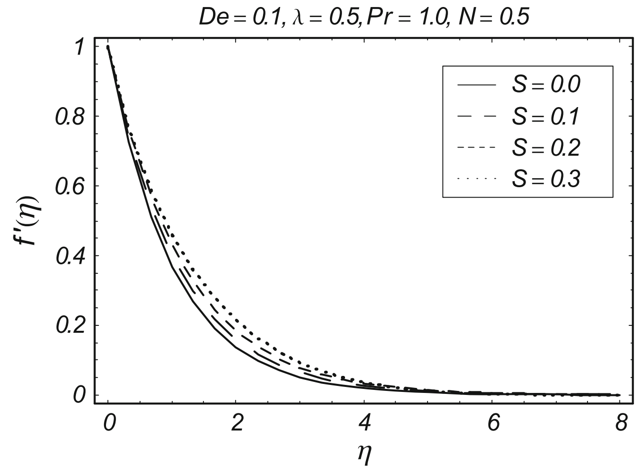

Fig. 6 Influence of S on $f'(\eta)$

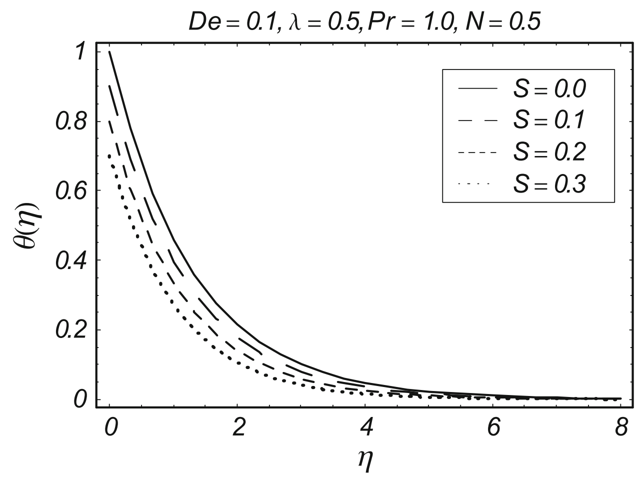

Fig. 7 Influence of S on $\theta(\eta)$

increase in *De* increases the relaxation time and thus decreases the velocity and boundary layer thickness. From Fig. 3, one can see that Deborah number has quite opposite effects on temperature in comparison to velocity. This reverse behavior is due to the relaxation time. In fact increase in Deborah number leads to an increase in the relaxation time. For larger relaxation time, the velocity is increased but temperature decreases. Hence, an increase in the Deborah number gives rise to the velocity and reduced the temperature. Figures 4 and 5 show that the velocity increases by increasing mixed convection parameter but the temperature decreases by increasing λ. This is because of the buoyancy force. The effects of thermal stratification parameter on velocity and temperature are observed from the Figs. 6 and 7. It is seen that both the velocity and temperature are decreasing functions of S. We also noticed that the variation in temperature is more significant when compared with velocity. This shows that the temperature decreases rapidly while the decrease in velocity is slow. There is a reduction in the effective convective potential between the surface and the ambient fluid for the increasing values of thermal stratification parameter. This reduction causes a decrease in the momentum and thermal boundary layer thicknesses. From Figs. 8 and 9, we see that both the velocity and temperature decrease by increasing Prandtl number. This is because of the fact that higher Prandtl number fluid has lower thermal diffusivity which decreases the temperature and thermal boundary layer thickness. Comparison of Figs. 8 and 9 shows that the thermal boundary layer thickness is more dominant than the velocity boundary layer thickness. The thermal radiation parameter N has similar effects on the velocity and temperature. Both the velocity and temperature increase by increasing N. An increase in the radiation parameter provides more heat to the fluid due to which the velocity and temperature are increased. It is also seen that an increase in temperature is

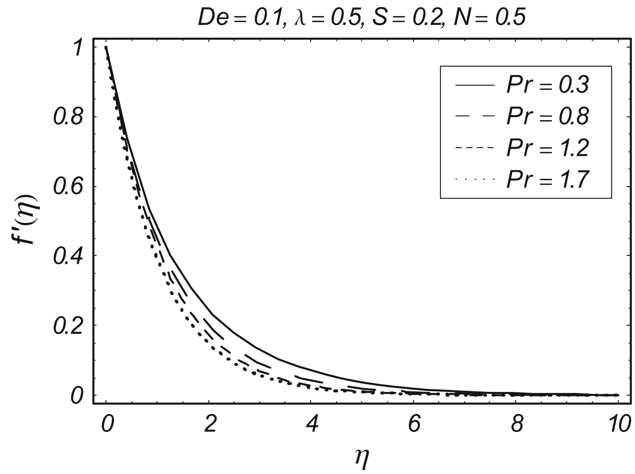

Fig. 8 Influence of Pr on $f'(\eta)$

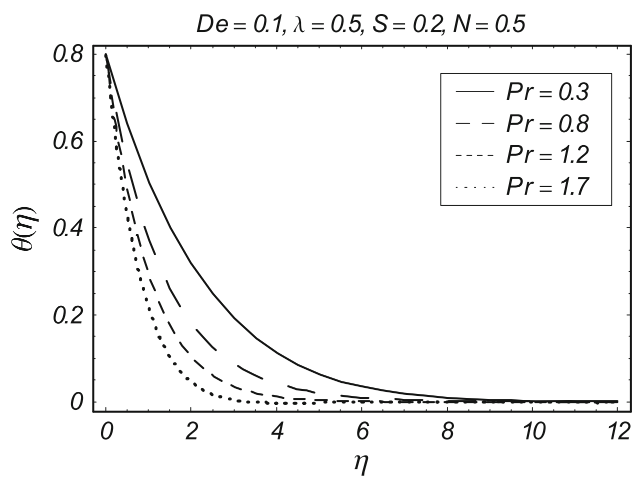

Fig. 9 Influence of Pr on $\theta(\eta)$

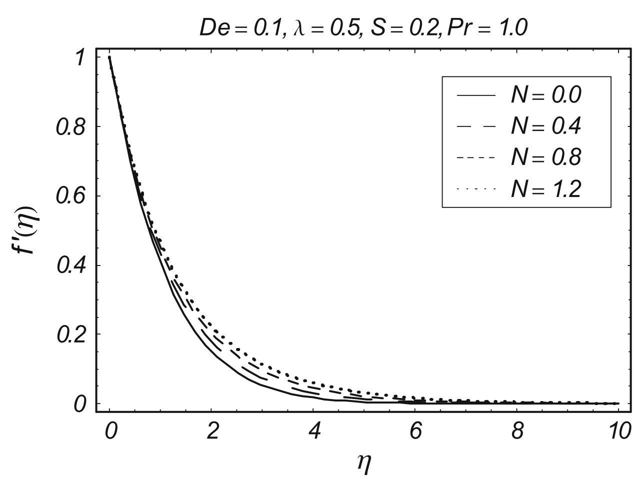

Fig. 10 Influence of N on $f'(\eta)$

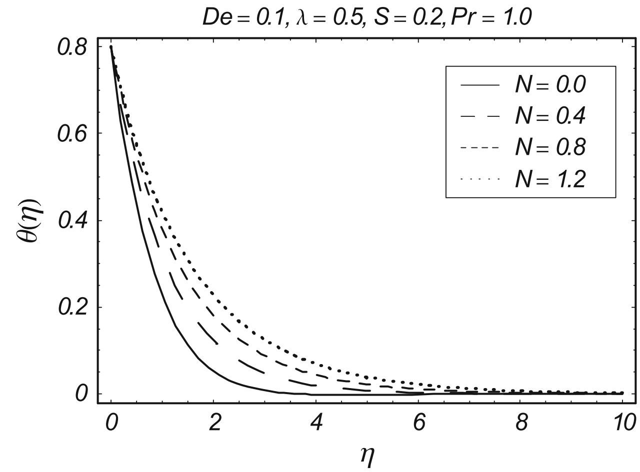

Fig. 11 Influence of N on $\theta(\eta)$

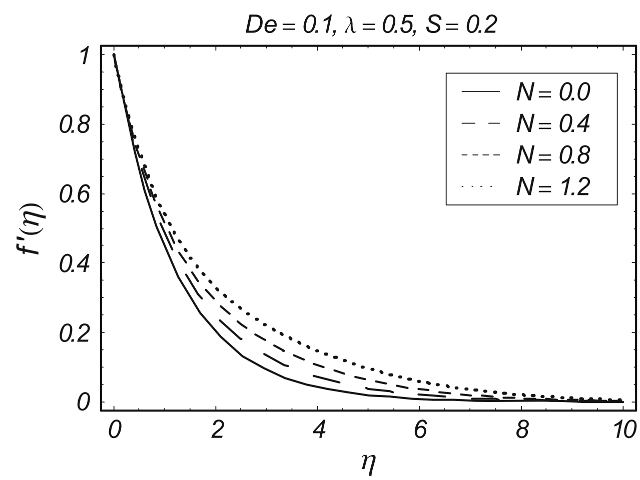

Fig. 12 Influence of N on $f'(\eta)$ when $Pr = 0.2$

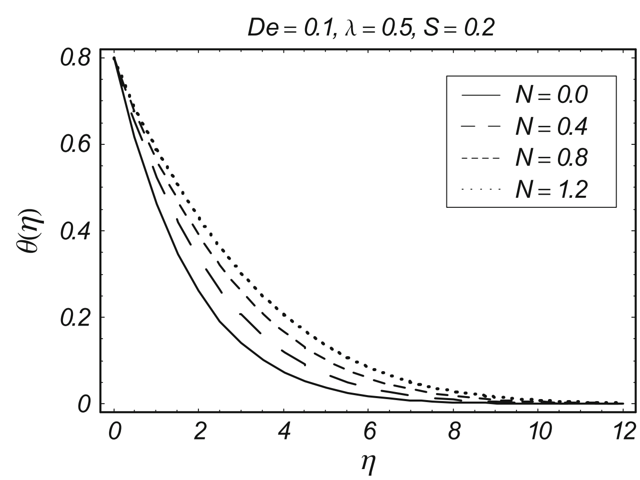

Fig. 13 Influence of N on $\theta(\eta)$ when $Pr = 0.2$

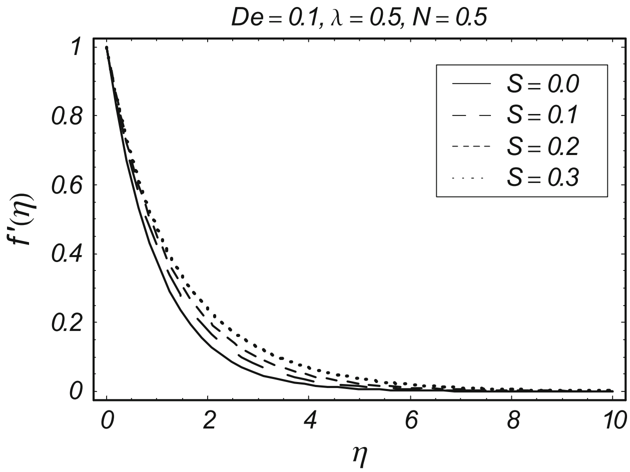

Fig. 14 Influence of S on $f'(\eta)$ when $Pr = 0.2$

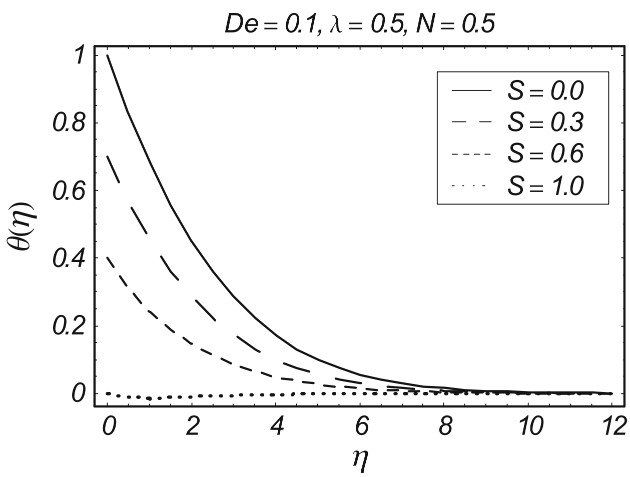

Fig. 15 Influence of S on $\theta(\eta)$ when $Pr = 0.2$

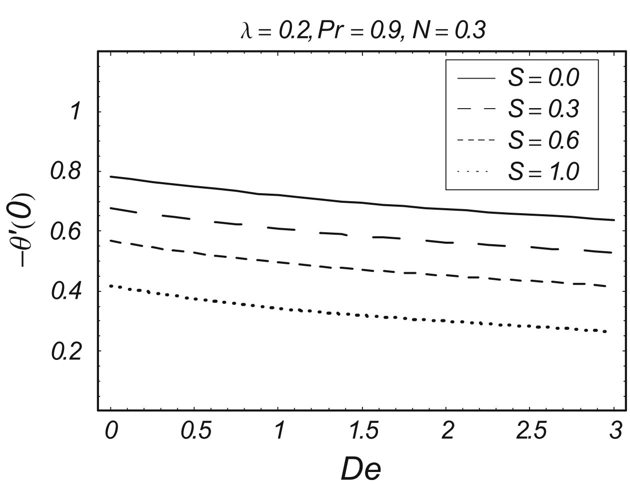

Fig. 16 Influence of S vs. De on $-\theta'(0)$

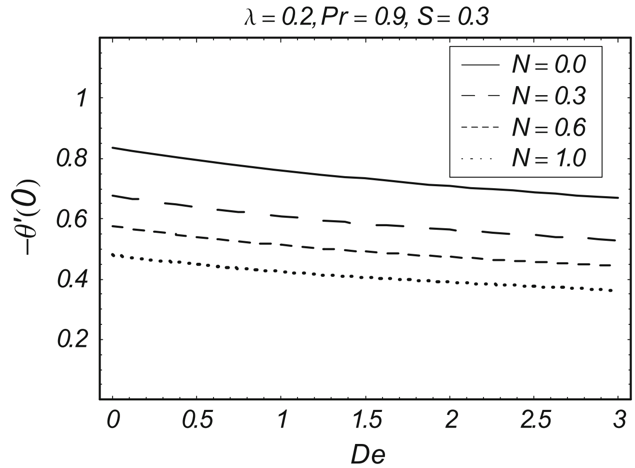

Fig. 17 Influence of N vs. De on $-\theta'(0)$

Table 1 Convergence of homotopy solution for different order of approximations when $De = 0.1$, $\lambda = 0.5$, $Pr = 1.0$, $S = 0.1$, $N = 0.5$, $\hbar_f = -0.7$ and $\hbar_\theta = -0.6$

Order of approximation	$-f''(0)$	$-\theta'(0)$
1	0.86000	0.75000
10	0.78217	0.73879
20	0.78207	0.73860
25	0.78208	0.73861
30	0.78208	0.73861
35	0.78208	0.73861

Table 2 Numerical values of local Nusselt number $-\theta'(0)$ for different values of De, λ, S, Pr and N

De	λ	Pr	S	N	$-\theta'(0)$
0.0	0.5	1.0	0.1	0.5	0.74632
0.3					0.72422
0.5					0.71112
0.1	0.0				0.67631
	0.6				0.74671
	1.0				0.77404
		0.4			0.43553
		0.9			0.69456
		1.3			0.86119
			0.0		0.77693
			0.2		0.69946
			0.3		0.65948
				0.0	0.99617
				0.4	0.77550
				0.7	0.67739

Table 3 Comparison values of $f''(0)$ and $\theta'(0)$ for different values of β when $\lambda = N = S = 0.0$

De	$-f''(0)$		$-\theta'(0)$	
	Vajravelu et al. [14]	Present results	Vajravelu et al. [14]	Present results
0.0	1.0001743	1.00000	1.0001743	1.00000
0.2	1.051975	1.051890	0.98009229	0.980077
0.4	1.1019475	1.101903	0.96078789	0.960805
0.6	1.1501625	1.150137	0.94231808	0.692263
0.8	1.1967279	1.196711	0.92469829	0.924694

rapid than velocity (see Figs. 10, 11). Figures 12 and 13 are plotted for the different values of radiation by considering smaller value of Prandtl number. Here we examined that the fluid velocity corresponding to $Pr = 1.0$ dies out quickly in comparison to the fluid velocity for $Pr = 0.2$. A comparison of Figs. 11 and 13 shows that increase in radiation increases the temperature for $Pr = 1.0$ and $Pr = 0.2$ but the temperature is higher for $Pr = 0.2$. Figure 14 shows the variations of S when $Pr = 0.2$ on the fluid velocity. The fluid velocity increased by increasing the values of S. From Figs. 6 and 14, we have seen that the fluid velocity is large for $Pr = 0.2$ when compared with the velocity for $Pr = 1.0$. From Fig. 15, one can see that the temperature is zero for $S = 1.0$. Also we see that the temperature decreases rapidly in Fig. 15 in comparison to Fig. 7. Figures 16 and 17 illustrate the effects of S and N vs. De on the local Nusselt number $-\theta'(0)$. The local Nusselt number reduced with an increase in S and N vs. De but the local Nusselt number corresponding to N is greater than the local Nusselt number for S.

Table 1 is prepared to see the convergent values and to find that how much deformations are required for the convergent series solutions. We see that the solutions for velocity and temperature start to repeat from 25th order of deformations. So it is concluded from this table that 25th order approximations are enough for the convergent series solutions of velocity and temperature. Numerical values of local Nusselt number $-\theta'(0)$ for different values of De, λ, Pr, S and N are examined in Table 2. The values of Nusselt number increase by increasing the values of Prandtl number and mixed convection parameter. Such values reduce by increasing the Deborah number, thermal stratification parameter and radiation parameter. Table 3 provides the comparison for different values of De on $f''(0)$ and $\theta'(0)$ with Vajravelu et al. [14]. Here we see that our homotopic solution has good agreement with that presented by Vajravelu et al. [14].

6 Conclusions

Influence of thermal stratification on the mixed convection flow of upper convected Maxwell fluid over a stretching sheet is explored. Similarity transformations are utilized for the reduction of partial differential equations into the ordinary differential equations. The governed nonlinear ordinary differential equations with the subjected boundary conditions are solved by homotopy analysis method. The main points of the presented study can be summed up as follows.

- Deborah number has reverse effects on the dimensionless velocity and temperature.
- There is decrease in both the velocity and temperature when thermal stratified parameter increases. However, the decrease in velocity is more significant than the temperature.
- Decrease in temperature and thermal boundary layer thickness is rapid when compared with an increase in velocity by increasing Prandtl number.
- The velocity and temperature increase by increasing the radiation parameter N.
- Values of local Nusselt number decrease when Deborah number and stratification parameter are increased.
- Increase in Prandtl number causes an increase in the values of $-\theta'(0)$.

Acknowledgments We are thankful to the reviewers for their useful suggestions and comments to improve the quality of manuscript. The research work of Dr. Al-Sulami was partially supported by the Deanship of Scientific Research (DSR), King Abdulaziz University, Saudi Arabia.

References

1. Jamil M, Fetecau C (2010) Helical flows of Maxwell fluid between coaxial cylinders with given shear stresses on the boundary. Nonlinear Anal Real World Appl 11:4302–4311
2. Athar M, Fetecau C, Kamran M, Sohail A, Imran M (2011) Exact solutions for unsteady axial Couette flow of a fractional Maxwell fluid due to an accelerated shear. Nonlinear Anal Model Control 16:135–151
3. Wang S, Tan WC (2011) Stability analysis of soret-driven double-diffusive convection of Maxwell fluid in a porous medium. Int J Heat Fluid Flow 32:88–94
4. Hayat T, Shehzad SA, Qasim M, Obaidat S (2011) Steady flow of Maxwell fluid with convective boundary conditions. Z Naturforsch 66a:417–422

5. Hayat T, Qasim M (2010) Influence of thermal radiation and Joule heating on MHD flow of a Maxwell fluid in the presence of thermophoresis. Int J Heat Mass Transf 53:4780−4788
6. Vajravelu K, Prasad KV, Sujatha A, Chiu-on NG (2012) MHD flow and mass transfer of chemically reactive upper convected Maxwell fluid past porous surface. Appl Math Mech Engl Ed 33:899–910
7. Haitao Q, Mingyu X (2007) Unsteady flow of viscoelastic fluid with fractional Maxwell model in a channel. Mech Res Commun 34:210–212
8. Tripathi D, Pandey SK, Das S (2010) Peristaltic flow of viscoelastic fluid with fractional Maxwell model through a channel. Appl Math Comput 215:3645–3654
9. Jamil M, Rauf A, Zafar AA, Khan NA (2011) New exact analytical solutions for Stokes' first problem of Maxwell fluid with fractional derivative approach. Comput Math Appl 62:1013–1023
10. Hayat T, Abbas Z (2008) Channel flow of a Maxwell fluid with chemical reaction. Z Angew Math Phys 59:124–144
11. Mukhopadhyay S (2010) Effects of slip on unsteady mixed convective flow and heat transfer past a stretching surface. Chin Phys Lett 27(12):124401
12. Turkyilmazoglu M (2011) Analytic heat and mass transfer of the mixed hydrodynamic/thermal slip MHD viscous flow over a stretching sheet. Int J Mech Sci 53:886–896
13. Noor NFM, Abbasbandy S, Hashim I (2012) Heat and mass transfer of thermophoretic MHD flow over an inclined radiate isothermal permeable surface in the presence of heat source/sink. Int J Heat Mass Transf 55:2122–2128
14. Vajravelu K, Prasad KV, Sujatha A (2011) Convection heat transfer in a Maxwell fluid at a non-isothermal surface. Cent Eur J Phys 9:807–815
15. Hayat T, Alsaedi A (2011) On thermal radiation and Joule heating effects in MHD flow of an Oldroyd-B fluid with thermophoresis. Arab J Sci Eng 36:1113–1124
16. Makinde OD (2012) Heat and mass transfer by MHD mixed convection stagnation point flow toward a vertical plate embedded in a highly porous medium with radiation and internal heat generation. Meccanica 47:1173–1184
17. Hayat T, Farooq M, Iqbal Z, Alsaedi A (2012) Mixed convection Falkner–Skan flow of a Maxwell fluid. J Heat Transf Trans ASME 134:114504
18. Kishore PM, Rajesh V, Verma SV (2010) Thermal stratification and viscous dissipation effects on MHD unsteady radiative natural convection flow past an infinite vertical accelerated plate embedded in a porous medium with variable surface temperature. Int J Appl Math Mech 6:1–18
19. Kulkarni AK, Jacobs HR, Hwang JJ (1986) Similarity solution for natural convection flow over an isothermal vertical wall immersed in a thermally stratified medium. Int J Heat Mass Transf 30:691–698
20. Thakhar HS, Chamkha AJ, Nath G (2002) Natural convection on a vertical cylinder embedded in a thermally stratified high-porosity medium. Int J Thermal Sci 41:83–93
21. Hossain MA, Saha SC, Gorla RSR (2005) Viscous dissipation effects on natural convection from a vertical plate with uniform surafce heat flux placed in a thermally stratified media. Int J Fluid Mech Res 32:269–280
22. Singh G, Sharma PR, Chamkha AJ (2010) Effect of thermally stratified ambient fluid on MHD convective flow along a moving non-isothermal vertical plate. Int J Phys Sci 5:208–215
23. Mukhopadhyay S, Ishak A (2012) Mixed convection flow along a stretching cylinder in a thermally stratified medium. J Appl Math Article ID 491695
24. Liao SJ (2003) Beyond perturbation: introduction to homotopy analysis method. Chapman and Hall, CRC Press, Boca Raton
25. Abbasbandy S (2011) Approximate analytical solutions to thermo-poroelastic equations by means of the iterated homotopy analysis method. Int J Comput Math 88:1763–1775
26. Rashidi MM, Mohimanian Pour SA, Abbasbandy S (2011) Analytic approximate solutions for heat transfer of a micropolar fluid through a porous medium with radiation. Commun Nonlinear Sci Numer Simulat 16:1874–1889
27. Liu C (2011) The essence of the generalized Taylor theorem as the foundation of the homotopy analysis method. Commun. Commun Nonlinear Sci Numer Simulat 16:1254–1262
28. Hayat T, Shehzad SA, Alsaedi A, Alhothuali MS (2012) Mixed convection stagnation point flow of Casson fluid with convective boundary conditions. Chin Phys Lett 29:114704
29. Bird RB, Armstrong RC, Hassager O (1987) Dynamics of polymeric liquids. Wiley, New York
30. Schichting H (1964) Boundary layer theory, 6th edn. McGraw-Hill, New York
31. Saha G, Sultana T, Saha S (2010) Effect of thermal radiation and heat generation on MHD flow past a uniformly heated vertical plate. Desalin Water Treat 16:57–65